Journal of Physiology (2002), **538.1**, *pp.* 65–77
DOI: 10.1013/jphysiol.2001.012685

www.jphysiol.org

Modulation by permeant ions of Mg^{2+} inhibition of NMDA-activated whole-cell currents in rat cortical neurons

Anqi Qian, Sergei M. Antonov * and Jon W. Johnson

*Department of Neuroscience, University of Pittsburgh, Pittsburgh, PA 15260, USA and *Sechenov Institute of Evolutionary Physiology and Biochemistry, Russian Academy of Science, St Petersburg 194223, Russia*

Whole-cell *N*-methyl-D-aspartate (NMDA)-activated currents were recorded from cultured rat cortical neurons. We report here a powerful effect of changing permeant ion concentrations on the voltage-dependent inhibition by external Mg^{2+} (Mg_o^{2+}) of these currents. Internal Cs^+ (Cs_i^+) affected Mg_o^{2+} inhibition of the NMDA-activated currents in a voltage-dependent manner. A decrease in Cs_i^+ concentration ($[Cs^+]_i$) from 125 to 8 mM reduced Mg_o^{2+} IC_{50} by 1.4-fold at −105 mV and by 11.5-fold at −15 mV. A decrease in external Na^+ (Na_o^+) concentration ($[Na^+]_o$) also reduced Mg_o^{2+} IC_{50}. This effect was voltage independent. A decrease in $[Na^+]_o$ from 140 to 70 mM reduced Mg_o^{2+} IC_{50} by 1.4-fold at −105 mV and by 1.6-fold at −15 mV. Varying external Ca^{2+} (Ca_o^{2+}) concentrations ($[Ca^{2+}]_o$) from 0.1 to1 mM did not affect Mg_o^{2+} inhibition, even though changing $[Ca^{2+}]_o$ in the same range strongly influenced the magnitude of NMDA-activated currents in the absence of Mg_o^{2+}. However, increasing $[Ca^{2+}]_o$ to higher concentrations (2–20 mM) greatly increased Mg_o^{2+} IC_{50} at hyperpolarized voltages. These data are consistent with a model in which Na_i^+ and Cs_i^+ modulate Mg_o^{2+} inhibition of NMDA-activated currents by occupying external permeant ion binding sites. The Mg_o^{2+} IC_{50} values reported here are similar to Mg_o^{2+} K_D values calculated from previous single-channel measurements of Mg_o^{2+} blocking kinetics. This similarity implies that Mg_o^{2+} does not affect gating while blocking the channel.

(Received 3 May 2001; accepted after revision 14 September 2001)
Corresponding author J. W. Johnson: Department of Neuroscience, 446 Crawford Hall, University of Pittsburgh, Pittsburgh, PA 15260, USA. Email: johnson@bns.pitt.edu

N-methyl-D-aspartate (NMDA) receptors are critically involved in physiological processes of both the developing and mature vertebrate central nervous system (CNS), including neuronal patterning formation (Iwasato *et al.* 2000) and learning and memory (Bliss & Collingridge, 1993; Tang *et al.* 1999). NMDA receptors are also implicated, directly or indirectly, in diseased states ranging from acute ischaemia-induced cell death to neurodegenerative disorders (Meldrum, 1992). Hence, regulation of NMDA receptors is crucial for proper functioning of the CNS.

Many substances modulate NMDA receptor function (McBain & Mayer, 1994; Dingledine *et al.* 1999). Magnesium is a particularly important modulator that exhibits a number of modes of action. It can act as a voltage-dependent channel blocker from both the external (Mayer *et al.* 1984; Nowak *et al.* 1984; Ascher & Nowak, 1988) and internal (Johnson & Ascher, 1990; Li-Smerin & Johnson, 1996) sides of the membrane. Magnesium can potentiate NMDA receptor activity by increasing the affinity of glycine for the NMDA receptor (Wang & MacDonald, 1995) or through a glycine-independent mechanism (Paoletti *et al.* 1995). Under certain conditions, Mg^{2+} also permeates the channel of NMDA receptors (Mayer & Westbrook, 1987; Stout *et al.* 1996; Antonov & Johnson, 1999; Zhu & Auerbach, 2001*a*, *b*).

The open-channel block of channels of NMDA receptors by Mg_o^{2+} has been extensively investigated. The widely accepted mechanism of external Mg^{2+} (Mg_o^{2+}) block involves Mg_o^{2+} binding to a discrete site within the open channel of NMDA receptors, obstructing current flow, and then unbinding to the external solution under most circumstances. The binding site is thought to be deep in the channel of the NMDA receptor, within the region where transmembrane voltage drop occurs. As a result, the affinity of Mg_o^{2+} for the binding site changes as a function of membrane voltage. At hyperpolarized membrane voltages, the probability of Mg_o^{2+} occupying the site is higher, hence the block is more pronounced.

While Mg_o^{2+} occupies the pore, it may interact with channel gating transitions. There are many ways in which a blocker can interact with gating. Sequential blockers, examples of which are thought to include 9-aminoacridine (Costa & Albuquerque, 1994; Benveniste & Mayer, 1995), IEM-1857 (Antonov & Johnson, 1996) and tetrapentylammonium (Sobolevsky *et al.* 1999), have the extreme

effect of preventing the channel gate from closing during block. Other channel blocks allow the gate to close and can be subsequently 'trapped' in the channel when the agonist is removed. Examples of such blockers of the NMDA receptor are MK-801 (Huettner & Bean, 1988), memantine (Blanpied *et al.* 1997; Chen & Lipton, 1997) and ketamine (MacDonald *et al.* 1987). The trapped blocker may also perturb gating parameters by affecting binding of agonists or gating transitions (Blanpied *et al.* 1997; Sobolevsky *et al.* 1999). The action of Mg_o^{2+} on gating is not yet clear. Several pieces of evidence suggest that there is little or no effect of block by Mg_o^{2+} on channel gating: (1) single-channel burst analysis of Mg_o^{2+} block indicated a clear departure from predictions for a sequential blocker (Nowak *et al.* 1984); (2) the NMDA receptor channel can close from the Mg_o^{2+} blocked state (Jahr & Stevens, 1990; Sobolevsky & Yelshansky, 2000); and (3) Mg_o^{2+} does not prevent NMDA or glycine dissociation (Benveniste & Mayer, 1995; Sobolevsky & Yelshansky, 2000). On the other hand, a reduction in the burst duration and a decrease in the channel opening frequency may indicate that channel closure is accelerated during block by Mg_o^{2+} (Nowak *et al.* 1984; Ascher & Nowak, 1988).

Several molecular constituents of the channel of NMDA receptors have been identified that influence Mg_o^{2+} block. Notably, the *N*-site, located at the tip of the M2 region, and its neighbouring asparagine of NR2 subunits are most likely the key residues that co-ordinate Mg_o^{2+} during block (Burnashev *et al.* 1992; Mori *et al.* 1992; Kupper *et al.* 1996; Wollmuth *et al.* 1998). Kuner & Schoepfer (1996) found that many other regions of the receptor also influence Mg_o^{2+} block. These regions probably help form the external and internal vestibules and the pore region (Kuner *et al.* 1996; Beck *et al.* 1999) and thus it is unlikely that they all contribute to the Mg^{2+} binding site. This diffuse distribution of structural elements responsible for Mg_o^{2+} block appears inconsistent with the idea that Mg_o^{2+} blocks at a discrete site within the channel. This discrepancy echos the long-existing puzzle of how Mg_o^{2+} block acquires its unusually strong voltage dependence.

An explanation of this puzzle was provided by recent single-channel studies (Antonov & Johnson, 1999; Zhu & Auerbach, 2001*a*, *b*) which demonstrated that permeant monovalent ions have a powerful effect on the kinetics of channel block and unblock by Mg_o^{2+}. These studies suggest that voltage-dependent binding of permeant monovalent ions to the external channel vestibule of NMDA receptors accentuate the voltage dependence of Mg_o^{2+} block.

In the work presented here, we investigated the effect of permeant ions on Mg_o^{2+} inhibition of whole-cell NMDA-activated currents. The goal is twofold. First, we characterized the relevance of the interaction between permeant ions and Mg_o^{2+} to current inhibition. The results demonstrate that the equilibrium constant of Mg_o^{2+} inhibition of macroscopic currents is regulated dramatically by the ionic environment of a neuron. Second, we compare the whole-cell data with predictions of the previously proposed model based on single-channel measurements (Antonov & Johnson, 1999). This comparison tests whether the model, which was derived from kinetic measurements made at low Mg_o^{2+} concentrations ($[Mg^{2+}]_o$), is adequate to explain Mg_o^{2+} inhibition of macroscopic currents at higher, more physiologically relevant $[Mg^{2+}]_o$. The good agreement between whole-cell measurements of IC_{50} and single-channel measurements of K_D also implies that Mg_o^{2+} block has no effect on channel gating. Preliminary versions of some of these results have been presented previously (Qian & Johnson, 1997, 1998).

METHODS

Cell culture

Primary cultures of cortical neurons were prepared as described by Li-Smerin & Johnson (1996). The procedure was approved by the Institutional Animal Care and Use Committee at the University of Pittsburgh. Briefly, 16-days-old pregnant Sprague-Dawley rats were killed by CO_2 inhalation. Brains from the embryos were removed and cerebral cortices were harvested. The cortical cells were dissociated enzymatically and plated at a density of 2×10^5 to 2.5×10^5 cells ml^{-1} onto 35 mm diameter plastic Petri dishes that contained glass coverslips, which either had been coated with poly-L-lysine or contained a glial cell feeder layer. Cells were used from 10 to 42 days after plating.

Solutions

Solutions were delivered through a five- or seven-barrel fast perfusion system, similar to the one described in Blanpied *et al.* (1997). Solution changes were accomplished by movements of barrels. Each barrel was connected to a gravity-fed reservoir of solution. At the output of the reservoir, a solenoid valve was used to turn solution flow on or off. The speed of flow was adjusted by varying the height of the reservoirs to ensure rapid and complete change of solution following movement of the barrels. With this system, a 98–99 % complete solution exchange typically occurs within 120 ms (Blanpied *et al.* 1997).

Solutions were prepared daily from frozen stocks. For external solutions, 0.2 μM tetrodotoxin was added. Currents were activated by 10 μM NMDA + 30 μM glycine (identified on Figures as NMDA). Strychnine (1 μM) was also included to prevent activation of the strychnine-sensitive glycine receptor. Magnesium concentrations from 1 μM to 3 mM were added to external solutions. To determine whether the contaminating $[Mg^{2+}]$ was sufficiently great to affect the final $[Mg^{2+}]$ of external solutions, we used an atomic absorption spectrophotometer (Perkin-Elmer 2380; Shelton, CT, USA) to measure $[Mg^{2+}]$. Contaminating $[Mg^{2+}]$ in the control external solution + 10 μM NMDA + 30 μM glycine was too low to be measured accurately, but we established that it must be less than 0.31 μM. Based on this low maximal level of contaminating Mg^{2+}, we did not use Mg^{2+} buffers (which in some cases may yield inaccurate final-free $[Mg^{2+}]$; Li-Smerin *et al.* 2001) or make corrections to Mg^{2+} concentrations. The abbreviations and contents of external bath solutions are (mM): '140 Na_o^+' solution (where Na_o^+ represents external Na^+), 140 NaCl,

1 $CaCl_2$, 2.8 KCl and 10 Hepes; '70 Na_o^+' solution, 70 NaCl, 140 sucrose, 0.5 $CaCl_2$, 2.8 KCl and 10 Hepes. The pH of external solutions was adjusted to between 7.1 and 7.2 using NaOH. In experiments in which external Ca^{2+} (Ca_o^{2+}) concentration ($[Ca^{2+}]_o$) was changed to 0.2, 0.5 or 2 mM (in 140 Na_o^+ solution) or to 0.1 mM (in 70 Na_o^+ solution), no other changes in solute concentration were made. When $[Ca^{2+}]_o$ was raised to 5 or 20 mM (in 70 Na_o^+ solution), the sucrose concentration was reduced to 125 or 80 mM, respectively.

Caesium was used as the principal intracellular permeant cation because it inhibits K^+ conductance in neurons, but is about as permeant through the channel of NMDA receptors as Na^+ and K^+ (Tsuzuki *et al.* 1994). The abbreviations and contents of the internal solutions are (mM): '125 Cs_i^+' solution, where Cs_i^+ represents internal Cs^+, 125 CsCl, 10 EGTA and 10 Hepes; '8 Cs_i^+' solution, 8 CsCl, 117 *N*-methyl-D-glucamine (NMDG), 10 EGTA and 10 Hepes. The pH of the internal solutions was adjusted to between 7.1 and 7.2 using CsOH or HCl.

NMDG was used to adjust the osmolality of the internal solutions because it maintains ionic strength while neither blocking nor permeating the channel (Villarroel *et al.* 1995). Sucrose was used for external solutions because no ionic substitute for Na^+ could be found that did not either block or permeate the channel from the external solution at the necessary concentration (Antonov *et al.* 1998). The junction potentials between the pipette and bath solution were measured and found to be 5 mV for the 140 Na_o^+/125 Cs_i^+ solution, −3 mV for the 140 Na_o^+/8 Cs_i^+solution, and −7 mV for the 70 Na_o^+/8 Cs_i^+ solution. All holding potentials were corrected for junction potentials. Ultra-pure salts were used when available. Tetrodotoxin was purchased from Alomone Labs (Jerusalem, Israel); all other chemicals were from Sigma Chemical Co. (St Louis, MO, USA).

Whole-cell recordings and analysis

Whole-cell patch-clamp recordings were performed at room temperature according to standard methods (Hamill *et al.* 1981). Pipettes (resistance of 2–5 MΩ) were pulled from borosilicate thin-walled glass capillaries with filaments (Warner Instrument Corp., Portland, OR, USA). Access resistance was compensated at 60–80 %. Currents were recorded with an Axopatch-1D or −200 amplifier, low-pass filtered at 10 kHz, digitized at 44 kHz with a Neuro-Corder (Cygnus Technology, Delaware Water Gap, PA, USA) and stored on videotape for later analysis. A continuous printout of the current trace on a chart recorder was used to monitor the quality of the recording and for later analysis. We imposed a delay of at least 5 min between breaking into the whole-cell configuration and the start of recording to allow for adequate exchange of the cytoplasm with the pipette solution. NMDA-activated currents in the absence and presence of Mg_o^{2+} were used to estimate Mg_o^{2+} IC_{50} from −105 to −15 mV at 10 mV increments. During each measurement, agonists were applied to obtain a steady-state current in the absence of Mg_o^{2+} ($I_{control}$). One or several different $[Mg^{2+}]_o$ were applied in the presence of agonists to obtain currents in the presence of Mg_o^{2+}(I_{Mg}); Mg_o^{2+} application was followed by a second measurement of $I_{control}$. Recordings were discarded if the amplitudes of the first and second steady-state $I_{control}$ differed by more than 12 %.

The steady-state whole-cell current amplitudes were measured either directly from the chart recorder output or using pCLAMP 6 (Axon Instruments, Union City, CA, USA). Similar results were obtained with either approach. Normalized current in the presence of Mg_o^{2+} at each voltage was calculated as a ratio of I_{Mg} to $I_{control}$ (represented as a percentage).

Millimolar Mg_o^{2+} can potentiate NMDA responses in a glycine- and voltage-independent manner (Paoletti *et al.* 1995). To

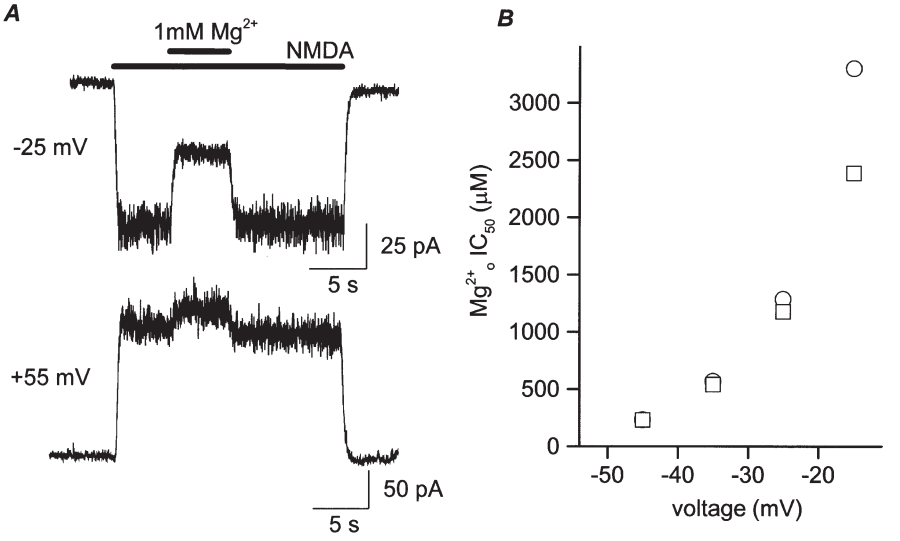

Figure 1. Correction for potentiation by Mg_o^{2+}

A, example of a cell in which the NMDA-activated current was potentiated by Mg_o^{2+}. Bars above the traces indicate times of agonist and Mg_o^{2+} application. At −25 mV, the inward current was inhibited by 1 mM Mg_o^{2+}; at +55 mV, 1 mM Mg_o^{2+} potentiated the outward current. *B*, calculated Mg_o^{2+} IC_{50} values before (○) and after (□) correction for Mg_o^{2+} potentiation are plotted here for comparison. At depolarized voltages, where Mg_o^{2+} IC_{50} reaches the millimolar range, Mg_o^{2+} potentiation leads to overestimation of IC_{50} values and exaggeration of the voltage dependence of Mg_o^{2+} inhibition.

accurately measure inhibition of NMDA-activated current by Mg_o^{2+}, $I_{Mg}/I_{control}$ was corrected for Mg_o^{2+} potentiation. We tested the potentiation only when $[Mg^{2+}]_o$ was 1 mM or higher because initial experiments indicated that 300 μM Mg_o^{2+} (the next highest $[Mg^{2+}]_o$ to 1 mM) showed negligible potentiation. Potentiation by Mg_o^{2+} was quantified by measuring $I_{Mg}/I_{control}$ at +35 or +55 mV. Then, $I_{Mg}/I_{control}$ measured at negative voltages was corrected for Mg_o^{2+} potentiation using the equation:

$$\text{Corrected fractional current} = 100\, I_{Mg}/(I_{control} A),$$

where corrected fractional current is expressed as a percentage and A is the value of $I_{Mg}/I_{control}$ measured at +35 or +55 mV in the same cell. Figure 1*A* shows a recording where potentiation by 1 mM Mg_o^{2+} was observed. At +55 mV, $I_{Mg}/I_{control}$ was 116 %; at −25 mV, $I_{Mg}/I_{control}$ was 48 % in the presence of 1 mM Mg_o^{2+}, with the corrected $I_{Mg}/I_{control}$ being 42 %. Mg_o^{2+} potentiation interfered with accurate measurements of IC_{50}, as shown in Fig. 1*B*, where corrected and uncorrected IC_{50} values are compared from −15 mV to −45 mV.

The IC_{50} of Mg_o^{2+} at each voltage was obtained by fitting $I_{Mg}/I_{control}$ at various Mg_o^{2+} concentrations using the following equation:

$$I_{Mg}/I_{control} = 100/[1 + ([Mg^{2+}]_o/IC_{50})^{n_H}].$$

IC_{50} and n_H (Hill coefficient) were free parameters in fitting and the result is expressed as a percentage. Curve fitting was performed using Origin 3.0 or 4.0 (Microcal Software, Northampton, MA, USA). All data points were used to obtain the IC_{50}, although the means were plotted for clarity in Figs 2*B* and 3*B*. Each IC_{50} value was based on $I_{Mg}/I_{control}$ measurements at 3–8 different $[Mg^{2+}]_o$ from 20–112 cells. Data are expressed as means ± S.E.M. Student's *t* test was used for statistical comparisons.

RESULTS

Effect of internal permeant ion on Mg_o^{2+} inhibition of NMDA-activated currents

We first investigated the effect of changing Cs_i^+ concentration ($[Cs^+]_i$) on Mg_o^{2+} inhibition of NMDA-activated whole-cell current. We compared Mg_o^{2+} inhibition of NMDA-activated currents in two sets of solutions, 140 Na_o^+/125 Cs_i^+ and 140 Na_o^+/8 Cs_i^+ solutions. Figure 2*A* shows current traces recorded at −95 mV (left) and −55 mV (right) for 125 Cs_i^+ (upper traces) and 8 Cs_i^+ (lower traces). At −95 mV, the two traces (with 125 and 8 Cs_i^+) exhibited similar values of $I_{Mg}/I_{control}$ at each $[Mg^{2+}]_o$. At −55 mV, Mg_o^{2+} inhibited NMDA-activated currents more effectively with 8 Cs_i^+.

To further quantify Mg_o^{2+} inhibition of NMDA-activated current with the 125 and 8 Cs_i^+ solutions, concentration–inhibition curves were constructed at each voltage tested. The IC_{50} of Mg_o^{2+} at each voltage was obtained by curve fitting of $I_{Mg}/I_{control}$ at various $[Mg^{2+}]_o$ as described in Methods. Examples of concentration–inhibition curves

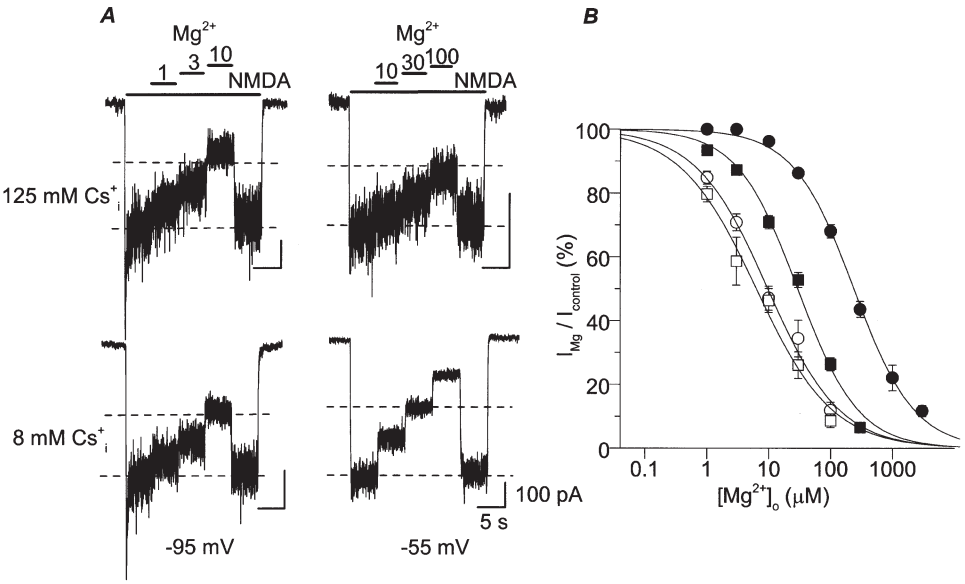

Figure 2. Effect of Cs_i^+ on inhibition by Mg_o^{2+} of NMDA-activated current

A, whole-cell NMDA-activated currents were inhibited by the indicated $[Mg^{2+}]_o$ (in μM). The $[Mg^{2+}]_o$ used were the same for upper and lower current traces. Bars above the traces show times of application of each solution. Each of the four current traces is from a different cell. At −95 mV (left), the values of $I_{Mg}/I_{control}$ were 80, 69 and 38 % for 125 Cs_i^+ (upper trace) and 85, 71 and 47 % for 8 Cs_i^+ (lower trace) in 1, 3 and 10 μM Mg_o^{2+}, respectively. At −55 mV (right), the values of $I_{Mg}/I_{control}$ were 91, 77 and 59 % for 125 Cs_i^+ (upper trace) and 73, 50 and 27 % for 8 Cs_i^+ (lower trace) in 10, 30 and 100 μM Mg_o^{2+}, respectively. The dashed lines indicate 50 and 100 % of $I_{control}$ to assist visual comparison among traces. *B*, examples of concentration–inhibition curves are shown. The symbol, solution, voltage and IC_{50} for each trace are: ○, 140 Na_o^+/125 Cs_i^+, −95 mV, 9.79 μM; □, 140 Na_o^+/8 Cs_i^+, −95 mV, 6.46 μM; ●, 140 Na_o^+/125 Cs_i^+, −45 mV, 232 μM; ■, 140 Na_o^+/8 Cs_i^+, −45 mV, 30.8 μM.

are shown in Fig. 2*B*. These examples demonstrate a general trend: IC_{50} was lower with 8 Cs^+_i than 125 Cs^+_i at each voltage, suggesting that Cs^+_i reduces Mg^{2+}_o inhibition of the NMDA receptor-mediated currents. In addition, this effect of changing $[Cs^+]_i$ was voltage dependent, since at −95 mV,Cs^+_i had a much weaker effect on Mg^{2+}_o IC_{50} than at −45 mV.

Effect of external permeant monovalent ion on Mg^{2+}_o inhibition of NMDA-activated currents

We next investigated how changing Na^+_o concentration ($[Na^+]_o$) affects Mg^{2+}_o inhibition of NMDA receptors. To minimize potential competition between Na^+_o and Cs^+_i (Antonov & Johnson, 1999), low $[Cs^+]_i$ was used in this series of experiments. Mg^{2+}_o inhibition of NMDA-activated currents was quantified with 70 Na^+_o/8 Cs^+_i and with 140 Na^+_o/8 Cs^+_i solutions. Figure 3*A* shows sample traces recorded at −95 mV (left) and −35 mV (right) with 140 Na^+_o (upper traces) and 70 Na^+_i (lower traces). At each voltage, increasing $[Na^+]_o$ reduced inhibition by Mg^{2+}_o. Voltage dependence of the effect of changing $[Na^+]_o$ on Mg^{2+}_o inhibition of NMDA-activated currents was not apparent.

Concentration–inhibition curves were constructed at each voltage tested with the 140 and the 70 Na^+_o solutions. Examples of these curves are shown in Fig. 3*B*. The IC_{50} of Mg^{2+}_o was lower when $[Na^+]_o$ was reduced, indicating that Mg^{2+}_o block becomes more pronounced in low $[Na^+]_o$. The shift of concentration–inhibition curves was comparable at both voltages.

Table 1. Measured Mg^{2+}_o IC_{50} values

Voltage (mV)	Mg^{2+}_o IC_{50} 140 Na^+_o/125 Cs^+_i (μM)	Mg^{2+}_o IC_{50} 140 Na^+_o/8 Cs^+_i (μM)	Mg^{2+}_o IC_{50} 70 Na^+_o/8 Cs^+_i (μM)
−15	2390	208	132
−25	1180	70.3	63.2
−35	541	56.3	35.8
−45	232	30.8	19.4
−55	116	24.9	12.3
−65	55.5	12.1	7.06
−75	41.5	12.1	5.89
−85	17.2	6.55	3.72
−95	9.79	6.46	2.98
−105	4.60	3.43	2.36

Mg^{2+}_o IC_{50} values are shown here for the three indicated solution combinations. Because each IC_{50} value was derived from a single fit to population data, no standard deviation or error is shown.

Comparison of the effects of internal and external permeant monovalent ions on Mg^{2+}_o inhibition of NMDA-activated currents

External magnesium IC_{50} values measured as described above are listed in Table 1 and plotted in Fig. 4 for all three solution combinations. The data demonstrate that changing permeant monovalent ion concentrations have a profound effect on the Mg^{2+}_o IC_{50}. For example, at −15 mV, a decrease in permeant ion concentration resulted in reduction of Mg^{2+}_o IC_{50} from 2390 μM (in 140 Na^+_o/125 Cs^+_i) to 208 μM (in 140 Na^+_o/8 Cs^+_i), and further to 132 μM (in 70 Na^+_o/8 Cs^+_i). The large variation in Mg^{2+}_o IC_{50} values in different solutions

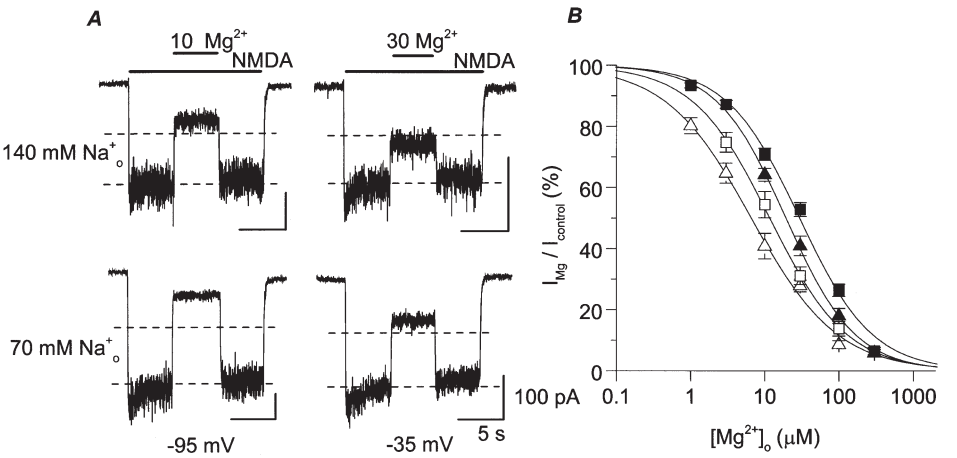

Figure 3. Effect of Na^+_o on inhibition by Mg^{2+}_o of NMDA-activated currents

A, whole-cell NMDA-activated currents were inhibited by the indicated $[Mg^{2+}]_o$ (in μM). The upper traces are from two different cells and the lower traces are from a third cell. At −95 mV (left), the values of $I_{Mg}/I_{control}$ were 36 % for 140 Na^+_o (upper trace) and 19 % for 70 Na^+_o (lower trace). At −35 mV (right), the values of $I_{Mg}/I_{control}$ were 60 % for 140 Na^+_o (upper trace) and 38 % for 70 Na^+_o (lower trace). Dashed lines, 50 and 100 % of $I_{control}$. *B*, examples of concentration–inhibition curves are shown. The symbol, solution, voltage and IC_{50} for each trace are: △, 70 Na^+_o/8 Cs^+_i, −85 mV, 3.72 μM; □, 140 Na^+_o/8 Cs^+_i, −85 mV, 6.55 μM; ▲, 70 Na^+_o/8 Cs^+_i, −45 mV, 19.4 μM; ■, 140 Na^+_o/8 Cs^+_i, −45 mV, 30.8 μM.

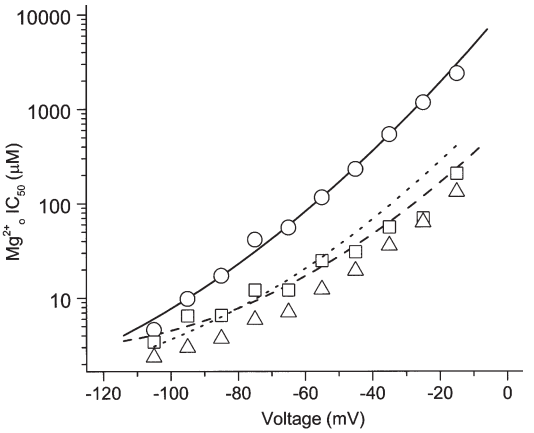

Figure 4. Voltage and permeant monovalent ion concentration dependence of Mg^{2+}_o IC_{50}

IC_{50} values (symbols); measured as shown in Figs 3 and 4, and quantitative predictions of Mg^{2+}_o K_D values (lines) made with the model of Antonov & Johnson (1999; see Fig. 8); are plotted as follows: 140 Na^+_o/125 Cs^+_i, ○ and —; 140 Na^+_o/8 Cs^+_i, □ and - - -; 70 Na^+_o/8 Cs^+_i, △ and ·····. The following equations were used with no free parameters to calculate the predictions of the model (V_m is membrane potential in mV; k_{Na} and k_{Cs} are in mM; $k_{-,o}$ and $k_{-,i}$ are in s^{-1}; and k_+ is in M^{-1} s^{-1}.

K_D (apparent dissociation constant for Mg^{2+}_o) = $k_{-,app}/k_{+,app}$,

$k_{-,app}$ (apparent Mg^{2+}_o unbinding rate) = $k_{-,o}/[(1 + [Na^+]_o/K_{Na})]^2 + k_{-,i}$,

$k_{+,app}$ (apparent Mg^{2+}_o binding rate) = $k_+/((1 + [Na^+]_o/K_{Na})(1 + [Na^+]_o/K_{Na} + [Cs^+]_i/K_{Cs}))$,

$k_{-,o}$ (intrinsic Mg^{2+}_o unbinding rate to external solution) = $1.10 \times 10^5 \exp(V_m/52.7)$,

$k_{-,i}$ (intrinsic Mg^{2+}_o unbinding rate to internal solution) = $61.8 \exp(-V_m/50.0)$,

k_+ (intrinsic Mg^{2+}_o binding rate) = $1.10 \times 10^9 \exp(-V_m/55.0)$,

K_{Na} ($[Na^+]$ at which each external site half occupied by Na^+) = 34.4,

K_{Cs} ($[Cs^+]$ at which external site half occupied by Cs^+) = $0.279 \exp(-V_m/21.0)$.

gradually diminished with hyperpolarization such that at −105 mV, the same decrease in permeant ion concentrations resulted in reduction of Mg^{2+}_o IC_{50} from 4.60 μM (in 140 Na^+_o/125 Cs^+_i) to 3.43 μM (in 140 Na^+_o/8 Cs^+_i), and further to 2.36 μM (in 70 Na^+_o/8 Cs^+_i). Changing permeant ion concentrations not only affected the magnitude of Mg^{2+}_o inhibition, it also altered the voltage dependence of Mg^{2+}_o inhibition, which was shallower in 140 Na^+_o/8 Cs^+_i and 70 Na^+_o/8 Cs^+_i than in 140 Na^+_o/125 Cs^+_i. The lines plotted in Fig. 4 are quantitative predictions from the kinetic model of Antonov & Johnson (1999). In this model, binding of permeant monovalent ions to sites in the external vestibule of the channel of NMDA receptors prevents Mg^{2+}_o block and unblock of the channel (see Discussion).

The effects on Mg^{2+}_o IC_{50} of changing $[Cs^+]_i$ and $[Na^+]_o$ exhibit a striking difference in voltage dependence. To

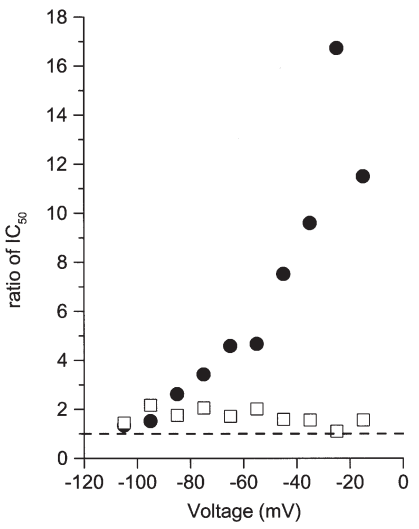

Figure 5. Comparison of voltage dependence of internal and external permeant monovalent ion effects on Mg^{2+}_o IC_{50}

Ratios of IC_{50} values measured in normal and low permeant ion concentrations are plotted as a function of voltage. ●, IC_{50} (in 140 Na^+_o/125 Cs^+_i)/IC_{50} (in 140 Na^+_o/8 Cs^+_i); □, IC_{50} (in 140 Na^+_o/8 Cs^+_i)/IC_{50} (in 70 Na^+_o/8 Cs^+_i). The dashed line marks a ratio of 1. The ratio for a change in $[Cs^+]_i$ increases with depolarization, while the ratio for a change in $[Na^+]_o$ shows no apparent voltage dependence.

illustrate this difference, the ratio of Mg_o^{2+} IC_{50} values measured in normal and low concentrations of each permeant monovalent ion is plotted as a function of voltage in Fig. 5 (see legend). Decreasing either $[Cs^+]_i$ or $[Na^+]_o$ reduced the Mg_o^{2+} IC_{50}, since all the ratios were greater than 1. At −105 mV, the effects of changing $[Cs^+]_i$ and $[Na^+]_o$ were comparable, with both ratios at 1.4. With depolarization, the effect of changing $[Cs^+]_i$ on Mg_o^{2+} IC_{50} became more pronounced. At −15 mV, decreasing $[Cs^+]_i$ caused an 11.5-fold reduction in Mg_o^{2+} IC_{50} value, while decreasing $[Na^+]_o$ resulted in a 1.6-fold reduction in the Mg_o^{2+} IC_{50} value.

Effect of $[Ca^{2+}]_o$ on Mg_o^{2+} inhibition of NMDA-activated currents

In the whole-cell experiments described so far, external solutions contained a $[Ca^{2+}]_o$ of 1 mM when 140 mM Na_o^+ was used and 0.5 mM when 70 mM Na_o^+ was used. As the channel of NMDA receptors is highly permeable to Ca_o^{2+} (MacDermott *et al.* 1986; Mayer & Westbrook, 1987; Ascher & Nowak, 1988; Burnashev *et al.* 1995), even these low $[Ca^{2+}]_o$ might have interfered with our measurements of the effects of Na_o^+ and Cs_i^+ on Mg_o^{2+} inhibition. Therefore, we next examined the effects on Mg_o^{2+} inhibition of variations of $[Ca^{2+}]_o$ around 1 mM.

Representative current traces recorded at several $[Ca^{2+}]_o$ are shown in Fig. 6*A*. The left panel shows current traces recorded in the same cell in 140 Na_o^+/125 Cs_i^+ at −65 mV, in normal $[Ca^{2+}]_o$ (top, 1 mM Ca_o^{2+}) and in low $[Ca^{2+}]_o$ (bottom, 0.2 mM Ca_o^{2+}). The right panel shows an example recorded in a second cell in 70 Na_o^+/8 Cs_i^+ at −45 mV, in normal $[Ca^{2+}]_o$ (top, 0.5 mM Ca_o^{2+}) and in low $[Ca^{2+}]_o$ (bottom, 0.1 mM Ca_o^{2+}). Within each trace, the $[Ca^{2+}]_o$ was the same in each solution (external solutions without agonists or Mg_o^{2+}, with only agonists, and with agonists and Mg_o^{2+}). When $[Ca^{2+}]_o$ was decreased fivefold, the steady-state $I_{control}$ became larger, as expected (Mayer & Westbrook, 1987; Ascher & Nowak, 1988), while inhibition by Mg_o^{2+} (reflected by $I_{Mg}/I_{control}$) was not noticeably affected.

Measurement of $I_{control}$ and $I_{Mg}/I_{control}$ at various $[Ca^{2+}]_o$ were normalized to values measured in normal $[Ca^{2+}]_o$

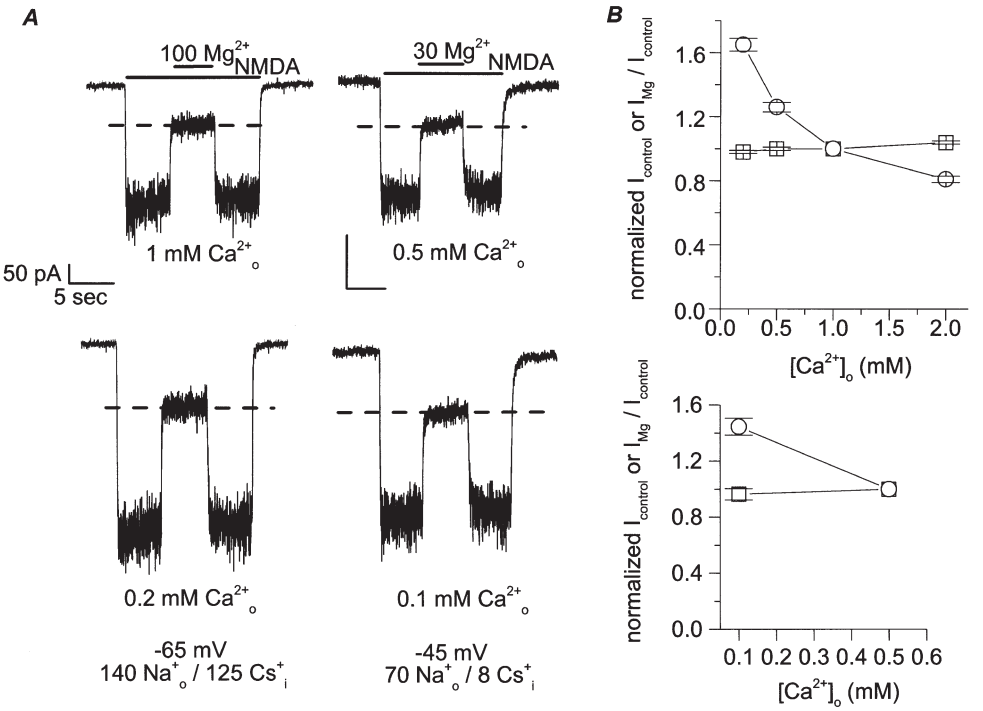

Figure 6. Effect of low $[Ca^{2+}]_o$ on NMDA-activated current and its inhibition by Mg_o^{2+}

A, sample traces are from recordings in the $[Ca^{2+}]_o$ indicated below each trace. The effect of Ca_o^{2+} is shown for experiments using 140 Na_o^+/125 Cs_i^+ at −65 mV (left two traces) and with 70 Na_o^+/8 Cs_i^+ at −45 mV (right two traces). Top traces are in normal $[Ca^{2+}]_o$ and bottom traces are in fivefold reduced $[Ca^{2+}]_o$. $[Mg^{2+}]_o$ was in μM. To assist visual data comparison, dashed lines are plotted at the value of $I_{Mg}/I_{control}$ measured in normal $[Ca^{2+}]_o$: 34.5 % in 140 Na_o^+/125 Cs_i^+ (left, top) and 36.8 % in 70 Na_o^+/8 Cs_i^+ (right, top) in *A*. The measured values of $I_{Mg}/I_{control}$ in low $[Ca^{2+}]_o$ are 35.1 % in 140 Na_o^+/125 Cs_i^+ (left, bottom) and 36.6 % in 70 Na_o^+/8 Cs_i^+ (right, bottom). *B*, $I_{control}$ (○) and $I_{Mg}/I_{control}$ (□) were measured in various $[Ca^{2+}]_o$; all data were normalized to values in normal $[Ca^{2+}]_o$ from the same cell (top, 1 mM Ca_o^{2+}; bottom, 0.5 mM Ca_o^{2+}) and were plotted as a function of $[Ca^{2+}]_o$ for 140 Na_o^+/125 Cs_i^+ (top) and for 70 Na_o^+/8 Cs_i^+(bottom). $I_{control}$ depended on $[Ca^{2+}]_o$, but $I_{Mg}/I_{control}$ was not affected by lowering $[Ca^{2+}]_o$, except for a small decrease in inhibition by Mg_o^{2+} at 2 mM Ca_o^{2+}. Plotted data are pooled from recordings performed at −45 and −65 mV in 140 Na_o^+/125 Cs_i^+ and at −45, −65 and −95 mV in 70 Na_o^+/8 Cs_i^+. At least three cells were used under each Ca_o^{2+}, Cs_i^+, Na_o^+ and voltage condition.

within the same cell. The mean normalized values are plotted as a function of $[Ca^{2+}]_o$ in Fig. 6*B*. The majority of the experiments were performed at −45 or −65 mV; for experiments in 70 Na_o^+/8 Cs_i^+, recordings were also made at −95 mV to rule out a voltage-dependent effect of changing $[Ca^{2+}]_o$ on $I_{Mg}/I_{control}$ measurements. None of the normalized $I_{Mg}/I_{control}$ values at any voltage was statistically different from 1 at $[Ca^{2+}]_o$ from 0.1 to 1 mM (the *P* values ranged from 0.12 to 0.96). Normalized $I_{control}$ values, on the other hand, increased with reduction of $[Ca^{2+}]_o$. Therefore, under the conditions used here, Ca_o^{2+} did not competitively influence the effects of permeant monovalent ions on Mg_o^{2+} inhibition.

We noticed a slight increase in $I_{Mg}/I_{control}$ value in 2 mM Ca_o^{2+} compared with normal $[Ca^{2+}]_o$ (ratio of 1.04 ± 0.01, $P < 0.005$). This observation, and the previous work of Mayer & Westbrook (1987) on relief of Mg_o^{2+} inhibition by Ca_o^{2+}, led us to examine the effects of higher $[Ca^{2+}]_o$. We tested whether 5 or 20 mM Ca_o^{2+} affected the Mg_o^{2+} IC_{50} of NMDA-activated currents. We used a hyperpolarized voltage (−95 mV) because, if the effect of Ca_o^{2+} is voltage dependent, its effect should be greater at more negative voltages (Mayer & Westbrook, 1987). 70 mM Na_o^+ and 8 mM Cs_i^+ were used to minimize potential competition from other permeant ions. Figure 7*A* shows current traces recorded in 5 mM Ca_o^{2+} (left) and 20 mM Ca_o^{2+} (right). Mg_o^{2+} inhibited NMDA-activated currents more effectively in 5 than in 20 mM Ca_o^{2+}.

Figure 7*B* shows Mg_o^{2+} IC_{50} measured at in 0.5, 5 and 20 mM Ca_o^{2+}. Increasing $[Ca^{2+}]_o$ greatly weakened Mg_o^{2+} inhibition. Changing $[Ca^{2+}]_o$ from 0.5 to 5 mM increased the Mg_o^{2+} IC_{50} by 4.3-fold, and further increasing $[Ca^{2+}]_o$ to 20 mM increased Mg_o^{2+} IC_{50} by an additional factor of 2.4.

DISCUSSION

In this study, the effects of the permeant ions Na_o^+, Cs_i^+ and Ca_o^{2+} on inhibition by Mg_o^{2+} of whole-cell NMDA-activated currents were investigated. The main findings are as follows. (1) Mg_o^{2+} inhibition of NMDA-activated currents can be profoundly modulated by changing permeant ion concentrations. (2) Decreasing $[Cs^+]_i$ decreased Mg_o^{2+} IC_{50} in a voltage-dependent manner. At hyperpolarized voltages, the Cs_i^+ effect was weak; at depolarized voltages, the Cs_i^+ effect was powerful. (3) Decreasing $[Na^+]_o$ weakly decreased the Mg_o^{2+} IC_{50} in a voltage-independent manner. (4) In contrast to the permeant monovalent ions, Ca_o^{2+} at concentrations up to those normally present (0.5 or 1 mM) had no effect on Mg_o^{2+} inhibition of NMDA-activated currents, while higher $[Ca^{2+}]_o$ appeared to greatly reduce Mg_o^{2+} inhibition.

Model of permeant monovalent ion effects on Mg_o^{2+} IC_{50}

Mechanistic interpretation of these results can be aided by a previous model based on a single-channel study of the effects of permeant monovalent ions on Mg_o^{2+} blocking kinetics (Antonov & Johnson, 1999). The characteristics of this model (schematized in Fig. 8) are as follows. (1) There are two binding sites for permeant monovalent ions in the external vestibule of the NMDA receptor. Na_o^+ can bind to one or both of these sites, while Cs_i^+ can occupy only one of the sites. (2) When either site is occupied by Na_o^+ or Cs_i^+, Mg_o^{2+} cannot enter to block the pore. (3) When Mg_o^{2+} is blocking the pore, Na_o^+ can occupy one or both of the external permeant monovalent ion sites and prevent Mg_o^{2+} from exiting to the external solution until Na_o^+ dissociates from the binding site. This aspect of the model is reminiscent of the ability of external K^+ to slow Ba^{2+}

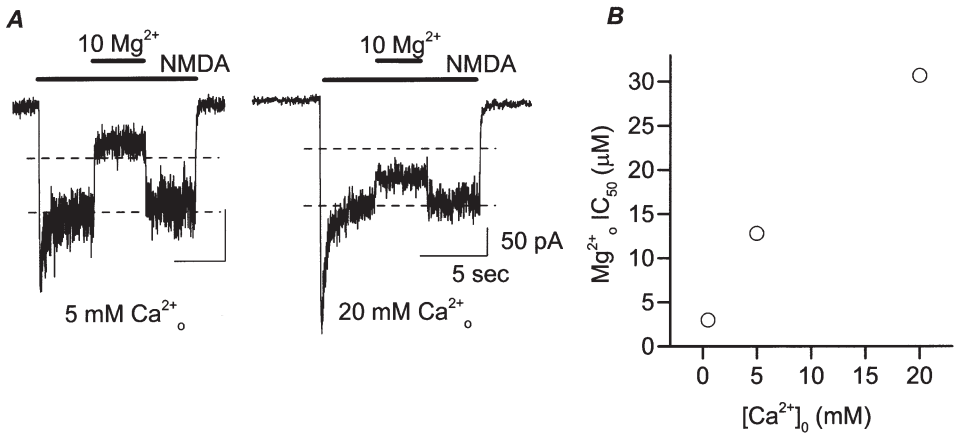

Figure 7. Effect of high $[Ca^{2+}]_o$ on inhibition by Mg_o^{2+} of NMDA-activated current

A, whole-cell NMDA-activated currents were inhibited by the indicated $[Mg^{2+}]_o$ (in μM) at −95 mV. The traces are from different cells. The values of $I_{Mg}/I_{control}$ were 32 % in 5 mM Ca_o^{2+} (left) and 71 % in 20 mM Ca_o^{2+} (right). Dashed lines indicate 50 and 100 % of $I_{control}$. *B*, whole-cell measurements of Mg_o^{2+} IC_{50} are plotted for three $[Ca^{2+}]_o$ (0.5, 5 and 20 mM Ca_o^{2+}). Data for 0.5 mM are replotted from Fig. 4. The Mg_o^{2+} IC_{50} values (in μM) are: 2.98, 12.8 and 30.7 in 0.5, 5 and 20 mM Ca_o^{2+}.

unblock by binding to the external lock-in site of Ca^{2+}-activated K^+ channels (Neyton & Miller, 1988; Jiang & MacKinnon, 2000). (4) Mg^{2+}_o can permeate the channel at a low, voltage-dependent rate. An alternative kinetic model (Zhu & Auerbach, 2001*a*, *b*) of permeant monovalent ion effects on Mg^{2+}_o block will be discussed below.

The model above provides an explanation for the high voltage dependence of Mg^{2+}_o inhibition of NMDA receptors. Cs^+_i reduces Mg^{2+}_o inhibition in a voltage-dependent manner by binding at the external permeant monovalent ion site. Since Cs^+_i must cross the entire membrane field to reach its binding site, Cs^+_i binding and its subsequent effect on Mg^{2+}_o inhibition is stronger at depolarized voltages. This voltage-dependent effect of Cs^+_i on Mg^{2+}_o inhibition exaggerates the voltage dependence of Mg^{2+}_o inhibition that results from the location of the blocking site in the membrane field (Woodhull, 1973).

Effect of Cs^+_i

To determine whether the model shown in Fig. 8 can explain the powerful effects of Cs^+_i on Mg^{2+}_o IC_{50}, we compared predicted values of Mg^{2+}_o K_D derived from the model to the IC_{50} values measured here. K_D values were predicted from the model as described in the legend of Fig. 4. Predictions were made with all parameters fixed at the values determined from previous single-channel experiments (Antonov & Johnson, 1999). Figure 4 compares the results of whole-cell experiments (symbols) to the model predictions (lines). The agreement was excellent for both 140 Na^+_o/125 Cs^+_i and 140 Na^+_o/8 Cs^+_i, supporting the accuracy of the model's description of the effect of Cs^+_i on Mg^{2+}_o inhibition. This agreement between data and model predictions also suggests that the model, which was derived from measurements made in a low $[Mg^{2+}]_o$ range (1–100 μM), is adequate to explain the blocking phenomenon at a more physiologically relevant (millimolar) $[Mg^{2+}]_o$ range.

Effect of Na^+_i

The effect of changing $[Na^+]_o$ on Mg^{2+}_o inhibition measured in whole-cell experiments and predicted by the model are also compared in Fig. 4. Three observations can be made. First, as the model predicts, changing $[Na^+]_o$ did affect Mg^{2+}_o inhibition of NMDA-activated currents. Second, the effect of changing $[Na^+]_o$ was small, which conforms with the model's prediction that the effect of $[Na^+]_o$ on Mg^{2+}_o unbinding rate (Fig. 8, states 7 and 8) should partially compensate for the effect on Mg^{2+}_o binding rate. Third, there were some differences between the model predictions and the whole-cell data. The model predicts that the effect of changing $[Na^+]_o$ on Mg^{2+}_o IC_{50} should be weakly voltage dependent, but there is no evidence of voltage dependency based on the whole-cell data. Despite

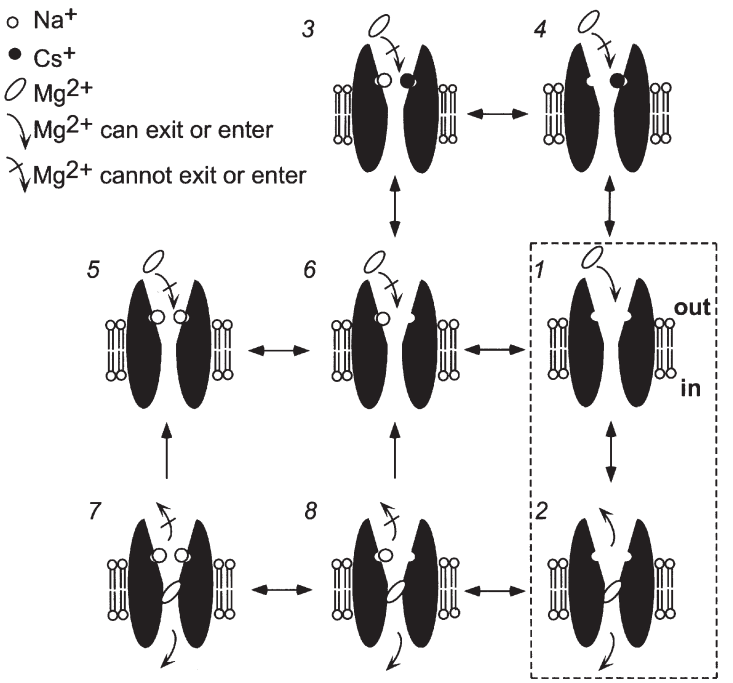

Figure 8. Diagram of model of Mg^{2+}_o block of NMDA receptors

The model based on single-channel measurement of Mg^{2+}_o block (Antonov & Johnson, 1999) is schematized here. States 1 and 2 illustrate Mg^{2+}_o block and unblock of the open channel of the NMDA receptor when permeant ions are not bound. States 3–6 illustrate states in which Na^+_o and/or Cs^+_i occupy the external permeant monovalent ion sites and prevent Mg^{2+}_o from entering the channel. States 7–8 illustrate that occupancy by Na^+_o of the external permeant monovalent ion site(s) prevents bound Mg^{2+}_o from exiting to the external solution, although permeation to the internal solution is still permitted.

this relatively small discrepancy between the model predictions and the measured Mg_o^{2+} IC_{50} values with 70 Na_o^+/8 Cs_i^+, the whole-cell data are consistent with the basic aspects of the model.

The weak voltage dependence of the $[Na^+]_o$ effect predicted by the model stems from competition between Na_o^+ and Cs_i^+ for one of the external permeant monovalent ion sites. At depolarized voltages, the principal effect of increasing $[Na^+]_o$ is to decrease the Mg_o^{2+} unblocking rate to the outside. This is because the probability of Cs_i^+ binding is high, and hence increasing $[Na^+]_o$ has very little additional effect on the Mg_o^{2+} blocking rate. At hyperpolarized voltages, since Cs_i^+ occupies the binding site only infrequently, will the addition of Na_o^+ reduce substantially the blocking as well as the unblocking rates of Mg_o^{2+}.

The reason for the small discrepancy is unclear. One possibility is that in 70 Na_o^+/8 Cs_i^+, the channel of NMDA receptors adopts a modified conformation that Mg_o^{2+} blocks with slightly different kinetics. Similarly, a $[K^+]$-dependent change in the conformation of the outer vestibule of K^+ channels that strongly affects block by TEA has been reported (Immke *et al.* 1999). Consistent with this hypothesis, model predictions fit the 70 Na_o^+/8 Cs_i^+ data better when we used a different set of parameter values, those of Zhu & Auerbach (2001*b*). Both 140 Na_o^+ data sets, however, are better described using parameter values shown in the legend of Fig. 4 .

Another possible explanation for the discrepancy with 70 Na_o^+/8 Cs_i^+ is that lowering $[Na^+]_o$ results in a change in the Mg_o^{2+} permeation rate. A previous study suggested that at 0 $[Na^+]_o$, Mg_o^{2+} permeation was greatly accelerated (Stout *et al.* 1996). Increased Mg_o^{2+} permeation could occur if, at low $[Na^+]_o$, a second Mg_o^{2+} can enter the channel vestibule, destabilize the blocking Mg_o^{2+}, and increase its rate of unblock to the internal solution.

We also attempted to explain our 70 Na_o^+/8 Cs_i^+ data by incorporating into our model an internal permeant ion binding site, as in the model of Zhu & Auerbach (2001*a*, *b*). Their model is based on single-channel studies of the effects of $[Na^+]$ and $[K^+]$ on the kinetics of Mg_o^{2+} block of recombinant NMDA receptors. Although there are many similarities between their model and the model summarized in Fig. 8, a prominent difference is that Zhu & Auerbach (2001*b*) proposed an additional internal ion binding site located 16 % into the voltage field from the internal side of the membrane. Occupancy of this site by K^+ was found to increase the unblocking rate of Mg_o^{2+}.

We did not expect that addition of an internal binding site to the model used here would yield better fits to the 70 Na_o^+/8 Cs_i^+ data because: (1) relatively little occupancy of the internal site would be expected at this low $[Cs^+]_i$; and (2) the internal site may selectively bind K^+, since Na^+ does not measurably interact with the site (Zhu & Auerbach, 2001*b*). The observation that changes in $[Cs^+]_i$ do not affect Mg_o^{2+} unbinding rate (Antonov & Johnson, 1999) suggests that Cs^+ may also have a low affinity for the site. To test the model with an internal permeant monovalent ion site, we fixed the electrical position of the internal site, and the Mg_o^{2+} unbinding rate with the site occupied, to the values specified in Zhu & Auerbach (2001*a*, *b*). The Cs^+ affinity for the internal site was left as a free parameter. When the other parameters were fixed at the values reported by Antonov & Johnson (1999; see Fig. 4 legend), no significant improvement in fits was observed, despite the addition of a free parameter. When the other parameters were fixed at the values reported by Zhu & Auerbach (2001*a*, *b*), an improvement in the fit of the 70 Na_o^+/8 Cs_i^+ data was observed. This improvement, however, was also observed when the Zhu & Auerbach (2001*a*, *b*) parameters were used without addition of an internal site, as described above. The fit to the 140 Na_o^+/8 Cs_i^+ data set remained much worse than that shown in Fig. 4, despite addition of a free parameter. Thus, the data in Fig. 4 do not provide clear support for an internal binding site for Cs_i^+.

It is possible that Cs^+ can bind to an internal site, but does not measurably affect Mg_o^{2+} block or unblock while bound. Previous work with organic channel blockers suggested the presence of an internal Cs^+ binding site located outside the voltage field (Antonov *et al.* 1998). It is not possible at present to determine whether this internal Cs^+ site is distinct from the internal K^+ site reported by Zhu & Auerbach (2001*b*).

Effect of $[Ca^{2+}]_o$

The powerful influence of Na_o^+ and Cs_i^+ on Mg_o^{2+} inhibition of NMDA-activated currents suggests the possibility that Ca_o^{2+} may compete with permeant monovalent cations for their external sites, and thereby affect Mg_o^{2+} inhibition as well. If, under the conditions of these experiments, there was significant binding of Ca_o^{2+} to the external permeant monovalent ion sites, then lowering $[Ca^{2+}]_o$ should have affected the Mg_o^{2+} IC_{50}. However, we observed that lowering $[Ca^{2+}]_o$ by a factor of 5 had no effect on $I_{Mg}/I_{control}$. This observation, in combination with previous single-channel observations (Antonov *et al.* 1998; Antonov & Johnson, 1999), suggests that Ca_o^{2+} does not compete with Na_o^+ or Cs_i^+ for their external binding sites under normal (low $[Ca^{2+}]_o$) conditions. NMDA-activated current in 0 Mg_o^{2+}, in contrast, did increase as $[Ca^{2+}]_o$ was reduced. This result is consistent with previous observations (Mayer & Westbrook, 1987; Ascher & Nowak, 1988) and indicates that the site at which Ca_o^{2+} binds with highest affinity during channel permeation is distinct from the external permeant monovalent ion sites.

At high $[Ca^{2+}]_o$, Mg_o^{2+} inhibition was strongly reduced at −95 mV, an observation consistent with the data of Mayer

& Westbrook (1987). It is possible that high $[Ca^{2+}]_o$ increases Mg^{2+}_o IC_{50} as a result of Ca^{2+}_o binding at a previously described binding site in the external portion of the NMDA-receptor channel (Premkumar & Auerbach, 1996; Sharma & Stevens, 1996). This external binding site might overlap with the external permeant monovalent ion sites. High Ca^{2+}_o may increase Mg^{2+}_o IC_{50} by slowing the apparent Mg^{2+}_o binding rate (similar to Na^+_o), by binding while Mg^{2+}_o blocks and increasing the Mg^{2+}_o permeation rate (as proposed by Mayer & Westbrook, 1987), or by a combination of these effects.

Mg^{2+}_o interaction with channel gating

The similarity between Mg^{2+}_o IC_{50} measured in whole-cell experiments and K_D (the ratio of Mg^{2+}_o unblocking and blocking rates) predicted from single-channel experiments also has implications for Mg^{2+}_o interaction with channel gating. IC_{50} and K_D values should differ if channel gating or agonist binding equilibria are modified when Mg^{2+}_o occupies the channel (Johnson & Qian, 2002). For example, if Mg^{2+}_o binding prevents the channel from closing, channel burst duration would be increased by Mg^{2+}_o. As a result, reduction of current flow by Mg^{2+}_o channel block would be partially offset by the lengthening of channel bursts, and the macroscopic IC_{50} would be larger than the K_D measured from single-channel experiments. The agreement between IC_{50} and K_D values is consistent with the idea that Mg^{2+}_o binding has no effect on the gating of NMDA receptors or on agonist unbinding. This conclusion was also reached by Sobolevsky & Yelshansky (2000), who proposed that Mg^{2+}_o block does not affect channel desensitization, channel closure or agonist dissociation. They further suggested that Mg^{2+}_o can be trapped in the closed channel. This idea was strongly supported by Amar *et al.* (2001) using an NMDA receptor with a high affinity Zn^{2+} blocking site generated by mutating the *N*-site amino acid to cysteine. The slow unbinding of Zn^{2+} from the mutated receptor permitted a clear demonstration that Zn^{2+} is trapped by closure of the channel. The observation that Mg^{2+}_o blocks without perturbing gating suggests that the selectivity filter, which is very close to the Mg^{2+}_o blocking site (Burnashev *et al.* 1992; Mori *et al.* 1992; Wollmuth *et al.* 1996, 1998), is relatively insulated from conformational changes associated with gating transitions. The observation that many channel blockers, probably including Mg^{2+}_o, can be trapped points to conformational changes associated with gating in a region well external to the *N*-site.

Physiological or pathological implications

The profound effects of permeant ions on Mg^{2+}_o inhibition may indicate a role for permeant ions in modulating cellular excitability under physiological or pathological conditions. Ion concentrations fluctuate significantly as a result of neuronal activity. Rose & Konnerth (2001), using two-photon Na^+ imaging, observed an increase of $[Na^+]$ in dendritic spines 100 mM in response to tetanic stimulation. More extreme fluctuations may occur in diseased states. Kager *et al.* (2000), for example, predicted an increase of over 50 % in the total internal ion concentration during modelled seizure discharge. Based on the results presented here, changes of this magnitude in total internal permeant cation concentration would lead to a substantial decrease in inhibition by Mg^{2+}_o. The result could be a great exacerbation of neuronal damage.

REFERENCES

Amar, M., Perin-Dureau, F. & Neyton, J. (2001). High-affinity Zn block in recombinant *N*-methyl-D-aspartate receptors with cysteine substitutions at the Q/R/N site. *Biophysical Journal* **81**, 107–116.

Antonov, S. M., Gmiro, V. E. & Johnson, J. W. (1998). Binding sites for permeant ions in the channel of NMDA receptors and their effects on channel block. *Nature Neuroscience* **1**, 451–461.

Antonov, S. M. & Johnson, J. W. (1996). Voltage-dependent interaction of open-channel blocking molecules with gating of NMDA receptors in rat cortical neurons. *Journal of Physiology* **493**, 425–445.

Antonov, S. M. & Johnson, J. W. (1999). Permeant ion regulation of *N*-methyl-D-aspartate receptor channel block by Mg^{2+}. *Proceedings of the National Academy of Sciences of the USA* **96**, 14571–14576.

Ascher, P. & Nowak, L. (1988). The role of divalent cations in the *N*-methyl-D-aspartate responses of mouse central neurones in culture. *Journal of Physiology* **399**, 247–266.

Beck, C., Wollmuth, L. P., Seeburg, P. H., Sakmann, B. & Kuner, T. (1999). NMDAR channel segments forming the extracellular vestibule inferred from the accessibility of substituted cysteines. *Neuron* **22**, 559–570.

Benveniste, M. & Mayer, M. L. (1995). Trapping of glutamate and glycine during open channel block of rat hippocampal neuron NMDA receptors by 9-aminoacridine. *Journal of Physiology* **483**, 367–384.

Blanpied, T. A., Boeckman, F. A., Aizenman, E. & Johnson, J. W. (1997). Trapping channel block of NMDA-activated responses by amantadine and memantine. *Journal of Neurophysiology* **77**, 309–323.

Bliss, T. V. P. & Collingridge, G. L. (1993). A synaptic model of memory: long-term potentiation in the hippocampus. *Nature* **361**, 31–39.

Burnashev, N., Schoepfer, R., Monyer, H., Ruppersberg, J., Gunther, W., Seeburg, P. & Sakmann, B. (1992). Control by asparagine residues of calcium permeability and magnesium blockade in the NMDA receptor. *Science* **257**, 1415–1419.

Burnashev, N., Zhou, Z., Neher, E. & Sakmann, B. (1995). Fractional calcium currents through recombinant GluR channels of the NMDA, AMPA and kainate receptor subtypes. *Journal of Physiology* **485**, 403–418.

Chen, H. S. & Lipton, S. A. (1997). Mechanism of memantine block of NMDA-activated channels in rat retinal ganglion cells: uncompetitive antagonism. *Journal of Physiology* **499**, 27–46.

Costa, A. C. S. & Albuquerque, E. X. (1994). Dynamics of the actions of tetrahydro-9-aminoacridine and 9-aminoacridine on glutamatergic currents: concentration-jump studies in cultured rat hippocampal neurons. *Journal of Pharmacology and Experimental Therapeutics* **268**, 503–514.

Dingledine, R., Borges, K., Bowie, D. & Traynelis, S. F. (1999). The glutamate receptor ion channels. *Pharmacological Reviews* **51**, 7–61.

Hamill, O. P., Marty, A., Neher, E., Sakmann, B. & Sigworth, F. J. (1981). Improved patch-clamp techniques for high-resolution current recording from cells and cell-free membrane patches. *Pflügers Archiv* **391**, 85–100.

Huettner, J. E. & Bean, B. P. (1988). Block of *N*-methyl-D-aspartate-activated current by the anticonvulsant MK-801: selective binding to open channels. *Proceedings of the National Academy of Sciences of the USA* **85**, 1307–1311.

Immke, D., Wood, M., Kiss, L. & Korn, S. J. (1999). Potassium-dependent changes in the conformation of the Kv2.1 potassium channel pore. *Journal of General Physiology* **113**, 819–836.

Iwasato, T., Datwani, A., Wolf, A. M., Nishiyama, H., Taguchi, Y., Tonegawa, S., Knopfel, T., Erzurumlu, R. S. & Itohara, S. (2000). Cortex-restricted disruption of NMDAR1 impairs neuronal patterns in the barrel cortex. *Nature* **406**, 726–731.

Jahr, C. E. & Stevens, C. F. (1990). A quantitative description of NMDA receptor-channel kinetic behavior. *Journal of Neuroscience* **10**, 1830–1837.

Jiang, Y. & MacKinnon, R. (2000). The barium site in a potassium channel by x-ray crystallography. *Journal of General Physiology* **115**, 269–272.

Johnson, J. W. & Ascher, P. (1990). Voltage-dependent block by intracellular Mg^{2+} of *N*-methyl-D-aspartate-activated channels. *Biophysical Journal* **57**, 1085–1090.

Johnson, J. W. & Qian, A. (2002). Interaction between channel blockers and channel gating of NMDA receptors. *Membrane and Cell Biology* (in the Press).

Kager, H., Wadman, W. J. & Somjen, G. G. (2000). Simulated seizures and spreading depression in a neuron model incorporating interstitial space and ion concentrations. *Journal of Neurophysiology* **84**, 495–512.

Kuner, T. & Schoepfer, R. (1996). Multiple structural elements determine subunit specificity of Mg^{2+} block in NMDA receptor channels. *Journal of Neuroscience* **16**, 3549–3558.

Kuner, T., Wollmuth, L. P., Karlin, A., Seeburg, P. H. & Sakmann, B. (1996). Structure of the NMDA receptor channel M2 segment inferred from the accessibility of substituted cysteines. *Neuron* **17**, 343–352.

Kupper, J., Ascher, P. & Neyton, J. (1996). Probing the pore region of recombinant *N*-methyl-D-aspartate channels using external and internal magnesium block. *Proceedings of the National Academy of Sciences of the USA* **93**, 8648–8653.

Li-Smerin, Y. & Johnson, J. W. (1996). Kinetics of the block by intracellular Mg^{2+} of the NMDA-activated channel in cultured rat neurons. *Journal of Physiology* **491**, 121–135.

Li-Smerin, Y., Levitan, E. S. & Johnson, J. W. (2001). Free intracellular Mg^{2+} concentration and inhibition of NMDA responses in cultured rat neurons. *Journal of Physiology* **533**, 729–743.

McBain, C. J. & Mayer, M. L. (1994). *N*-methyl-D-aspartic acid receptor structure and function. *Physiological Reviews* **74**, 723–760.

MacDermott, A. B., Mayer, M. L., Westbrook, G. L., Smith, S. J. & Barker, J. L. (1986). NMDA-receptor activation increases cytoplasmic calcium concentration in cultured spinal cord neurones. *Nature* **321**, 519–522.

MacDonald, J. F., Miljkovic, Z. & Pennefather, P. (1987). Use-dependent block of excitatory amino acid currents in cultured neurons by ketamine. *Journal of Neurophysiology* **58**, 251–266.

Mayer, M. L. & Westbrook, G. L. (1987). Permeation and block of *N*-methyl-D-aspartic acid receptor channels by divalent cations in mouse cultured central neurones. *Journal of Physiology* **394**, 501–527.

Mayer, M. L., Westbrook, G. L. & Guthrie, P. B. (1984). Voltage-dependent block by Mg^{2+} of NMDA responses in spinal cord neurones. *Nature* **309**, 261–263.

Meldrum, B. S. (1992). Excitatory amino acid receptors and disease. *Current Opinion in Neurology and Neurosurgery* **5**, 508–513.

Mori, H., Masaki, H., Yamakura, T. & Mishina, M. (1992). Identification by mutagenesis of a Mg^{2+}-block site of the NMDA receptor channel. *Nature* **358**, 673–675.

Neyton, J. & Miller, C. (1988). Potassium blocks barium permeation through a calcium-activated potassium channel. *Journal of General Physiology* **92**, 549–567.

Nowak, L., Bregestovski, P., Ascher, P., Herbet, A. & Prochiantz, A. (1984). Magnesium gates glutamate-activated channels in mouse central neurones. *Nature* **307**, 462–465.

Paoletti, P., Neyton, J. & Ascher, P. (1995). Glycine-independent and subunit-specific potentiation of NMDA responses by extracellular Mg^{2+}. *Neuron* **15**, 1109–1120.

Premkumar, L. S. & Auerbach, A. (1996). Identification of a high affinity divalent cation binding site near the entrance of the NMDA receptor channel. *Neuron* **16**, 869–880.

Qian, A. & Johnson, J. W. (1997). Internal permeant cations affect inhibition of NMDA-activated currents by external Mg^{2+}. *Society for Neuroscience Abstracts* **23**, 1, 243, 375.2.

Qian, A. & Johnson, J. W. (1998). External permeant cations affect inhibition of NMDA-activated currents by external Mg^{2+}. *Society for Neuroscience Abstracts* **24**, 1, 343.

Rose, C. R. & Konnerth, A. (2001). NMDA receptor-mediated Na^{+} signals in spines and dendrites. *The Journal of Neuroscience* **21**, 4207–4214.

Sharma, G. & Stevens, C. F. (1996). Interactions between two divalent ion binding sites in *N*-methyl-D-aspartate receptor channels. *Proceedings of the National Academy of Sciences of the USA* **93**, 14170–14175.

Sobolevsky, A. I., Koshelev, S. G. & Khodorov, B. I. (1999). Probing of NMDA channels with fast blockers. *The Journal of Neuroscience* **19**, 10611–10626.

Sobolevsky, A. I. & Yelshansky, M. V. (2000). The trapping block of NMDA receptor channels in acutely isolated rat hippocampal neurones. *Journal of Physiology* **526**, 493–506.

Stout, A. K., Li-Smerin, Y., Johnson, J. W. & Reynolds, I. J. (1996). Mechanisms of glutamate-stimulated Mg^{2+} influx and subsequent Mg^{2+} efflux in rat forebrain neurones in culture. *Journal of Physiology* **492**, 641–657.

Tang, Y. P., Shimizu, E., Dube, G. R., Rampon, C., Kerchner, G. A., Zhuo, M., Liu, G. & Tsien, J. Z. (1999). Genetic enhancement of learning and memory in mice. *Nature* **401**, 63–69.

Tsuzuki, K., Mochizuki, S., Iino, M., Mori, H., Mishina, M. & Ozawa, S. (1994). Ion permeation properties of the cloned mouse $\epsilon 2/\zeta 1$ NMDA receptor channel. *Molecular Brain Research* **26**, 37–46.

Villarroel, A., Burnashev, N. & Sakmann, B. (1995). Dimensions of the narrow portion of a recombinant NMDA receptor channel. *Biophysical Journal* **68**, 866–875.

Wang, L. Y. & Macdonald, J. F. (1995). Modulation by magnesium of the affinity of NMDA receptors for glycine in murine hippocampal neurones. *Journal of Physiology* **486**, 83–95.

Wollmuth, L. P., Kuner, T. & Sakmann, B. (1998). Adjacent asparagines in the NR2-subunit of the NMDA receptor channel control the voltage-dependent block by extracellular Mg^{2+}. *Journal of Physiology* **506**, 13–32.

Wollmuth, L. P., Kuner, T., Seeburg, P. H. & Sakmann, B.(1996). Differential contribution of the NR1- and NR2A-subunits to the selectivity filter of recombinant NMDA receptor channels. *Journal of Physiology* **491**, 779–797.

Woodhull, A. M. (1973). Ionic blockage of sodium channels in nerve. *The Journal of General Physiology* **61**, 687–708.

Zhu, Y. & Auerbach, A. (2001*a*). Na^+ occupancy and Mg^{2+} block of the *N*-methyl-D-aspartate receptor channel. *Journal of General Physiology* **117**, 275–286.

Zhu, Y. & Auerbach, A. (2001*b*). K^+ occupancy of the *N*-methyl-D-aspartate receptor channel probed by Mg^{2+} block. *Journal of General Physiology* **117**, 287–298.

Acknowledgements

The authors thank Juliann Jaumotte for her excellent skills in preparing the primary rat cortical culture and Dr Paul Rasmussen for his generous help with measurements of Mg^{2+} contamination. This work was supported by NIMH grants MH45817 and MH00944 to J. W. J. and Training Grant T32 MH18273 and Predoctoral NRSA MH12476 to A. Q.